Free Vibration Analysis of Launcher Structure Using 1D Refined Models

(Final report)

Naomi Luglio*, Joseph Morlier†
*Institut Supérieur de l'Aéronautique et de l'Espace (ISAE-SUPAERO), 31400 Toulouse, FRANCE
Email: {naomi.luglio}@student.isae-supaero.fr
†Institut Supérieur de l'Aéronautique et de l'Espace (ISAE-SUPAERO), 31400 Toulouse, FRANCE
Email: joseph.morlier@isae-supaero.fr

***Abstract*—This study has been performed for a future application to a reusable lunar launcher in the perspective of NASA's new project of a Lunar Orbital Platform-Gateway. In order to carry out this project, a reusable launcher will be required to deliver an certain payload from the moon to the lunar station and return. A fundamental step of this launcher project will certainly be its dynamic study. In this contest this paper uses different finite element approaches to carry out the free vibration analysis of a simplified model of a launcher. The 1D refined models, that are used in the present work, are based on the Carrera Unified Formulation (CUF), which assumes a variable kinematic displacement field over the cross-sections of the beam. Thanks to the compact form of the displacement field approximation, governing equations are written in terms of fundamental matrices. The frequencies and the natural modes obtained using the refined one-dimensional (1D) beam model are compared to those obtained by a commercial finite element software.**

I. Context

Launchers have been and will be essential for past and future space exploration as well as for placing satellites in orbit in order to provide communications and to observe the Earth. Moreover, NASA investment on a new project increased the interest in the study of launchers structure. In fact, the **Lunar Orbital Platform-Gateway** (fig. 1) is an international project led by NASA whose main purpose is to create a lunar-orbit space station. In this context, supplies will have to be transferred by a vehicle from the surface of the Moon to a Lunar Orbit: that is the reason for a recently increased interest in a reusable launcher that would be able to deliver a given payload from the surface of the Moon to lunar orbit and return.

Launchers are made up of reinforced thin-walled structures that are very complex to model and that must survive under severe loading and environmental conditions. Therefore, it is necessary to develop advanced numerical tools to reduce the computational cost of the analysis often required during structural design.

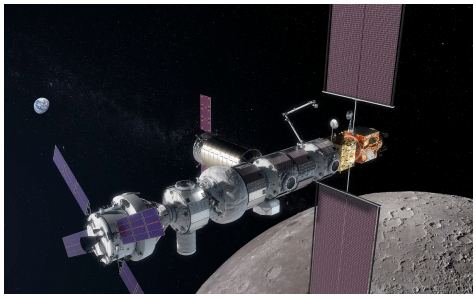

Figure 1. Artist's concept of Lunar Orbital Platform-Gateway orbiting the Moon.

II. Bibliography search

Computational tools have been used since the sixties to predict the dynamic characteristic of rockets and launchers. At that time, computers were not sufficiently powerful for carrying out a very complex dynamic analysis. Modal synthesis or component mode techniques were thus widely used: large structures were divided into substructures that were simpler and less computationally demanding to analyse: each substructure was first analysed separately, and then equilibrium equations at the boundaries were used to guarantee the congruence between components. In 1963, Przemieniecki [8] introduced a matrix approach to evaluate stresses and deflections in an aircraft structure composed of several substructural components. In a similar way, in 1965 Hurty [7] carried out a dynamic analysis of complex systems by using component modes approach. Nowadays, very fast computers have allowed the dynamic analysis of

even complex structures. However, as these analysis have a significant computational cost, it would be useful to dispose of a tool able to provide enough precise results with a lower number of degrees of freedom. In this sense, the Refined 1D Model could be very attractive. The Refined 1D method taken into consideration in this paper is based on the *Carrera Unified Formulation* (CUF) that splits the displacement into two components, one along the beam axis and one over its cross-section. Both Taylor expansions (TE) and Lagrange expansions (LE) can be used to describe the displacement over the cross-section. This formulation has been derived first for plates and shells [5] and then extended to beams with solid and thin-walled cross-sections [4] [1] [6]. Through a concise and compact notation for the displacement field, the governing differential equations are reduced to a 'fundamental nucleo' whose form does not depend on the approximation order. The latter, consequently, can be considered as a free parameter of the method. Classical models, such as the Euler-Bernoulli beam model, can be obtained as a particular case of this general formulation The finite element method is used to solve the problem along the longitudinal axis. Refined 1D Model based on *Carrera Unified Formulation* should be able to provide a solution similar to the 3D FEM solution but with a lower computational cost [2] [3]. This paper is organised as follows: the first section gives a clear illustration of the 1D Refined Method based on CUF formulation, while the second section compares several results obtained varying the approximation order. Finally, the considered method is applied to a simplification of launcher's structure. We are currently applying this formulation to a reusable lunar launcher model. Further studies could take into account composite materials and gravity force.

III. Refined one-dimensional models

This section introduces a unified formulation for refined 1D models. Further information could be found in the reference [3].

We suppose to dial with a structure whose the longitudinal axis is *x-axis* while plane (y, z) defines its cross-section.

The displacement vector $u(x, y, z)$ can be expressed through its components u_x, u_y and u_z.

$$u = \{u_x, u_y, u_z\}^T \tag{1}$$

Similarly, stress σ and deformation ϵ can be expressed as follows:

$$\sigma = \{\sigma_{xx}, \sigma_{yy}, \sigma_{zz}, \sigma_{xz}, \sigma_{yz}, \sigma_{xy}\}^T \tag{2}$$

$$\epsilon = \{\epsilon_{xx}, \epsilon_{yy}, \epsilon_{zz}, \epsilon_{xz}, \epsilon_{yz}, \epsilon_{xy}\}^T \tag{3}$$

Linear strain-displacement relations are considered:

$$\epsilon = \begin{bmatrix} \frac{\delta}{\delta x} & 0 & 0 \\ 0 & \frac{\delta}{\delta y} & 0 \\ 0 & 0 & \frac{\delta}{\delta z} \\ \frac{\delta}{\delta z} & 0 & \frac{\delta}{\delta x} \\ 0 & \frac{\delta}{\delta z} & \frac{\delta}{\delta y} \\ \frac{\delta}{\delta y} & \frac{\delta}{\delta x} & 0 \end{bmatrix} = [D]u \tag{4}$$

where $[D]$ is a differential operator. Hooke's law can be used to derive the stress field:

$$\sigma = [C]\epsilon \tag{5}$$

where $[C]$, for an isotropic material, is given by the following equation:

$$\sigma = \begin{bmatrix} \frac{1}{E} & -\frac{\nu}{E} & -\frac{\nu}{E} & 0 & 0 & 0 \\ -\frac{\nu}{E} & \frac{1}{E} & -\frac{\nu}{E} & 0 & 0 & 0 \\ -\frac{\nu}{E} & -\frac{\nu}{E} & \frac{1}{E} & 0 & 0 & 0 \\ 0 & 0 & 0 & \frac{1}{G} & 0 & 0 \\ 0 & 0 & 0 & 0 & \frac{1}{G} & 0 \\ 0 & 0 & 0 & 0 & 0 & \frac{1}{G} \end{bmatrix}^{-1} \epsilon \tag{6}$$

with E, τ and G that are respectively the Young's module, the Poisson ratio and the Shear Elastic Constant of the considered material.

A. Refined one-dimensional model

According to *Carrera Unified Formulation* (CUF), the displacement is split into two contributions: a function expansion $F_\tau(y, z)$ over the cross section and the contribution $u_\tau(x)$ along the longitudinal axis:

$$u = F_\tau(y, z)u_\tau(x) \tag{7}$$

Index τ ranges from one to the number M of terms of the expansion depending on y and z coordinates. According to Einstein notation, the repeated subscript τ indicates summation. The choice of F_τ is arbitrary: different base functions of any order can be taken into account to model the displacement field of a structure above its cross-section. Consequently, both Taylor and Lagrange expansions can be used as F_τ.

Table I
TAYLOR-LIKE POLYNOMIALS

N	M	F_τ
0	1	$F_1 = 1$
1	3	$F_2 = y$; $F_3 = z$
2	6	$F_4 = y^2$; $F_5 = yz$; $F_6 = z^2$
3	10	$F_7 = y^3$; $F_8 = y^2 z$;$F_9 = yz^2$; $F_10 = z^3$
N	$(N+1)(N+2)/2$	$F_{(N^2+N+2)/2} = y^N$ ... $F_{(N+1)(N+2)/2} = z^N$

B. Taylor expansions

Taylor-like polynomials consist of 2D base $y^i z^j$ functions, where i and j are positive integers.

For instance, the displacement field of the second-order model TE2 (N=2, M=6) is expressed as:

$$u_x(x,y,z) = u_{x_1} + yu_{x_2} + zu_{x_3} + y^2 u_{x_4} + yzu_{x_5} + z^2 u_{x_6} \tag{8}$$

$$u_y(x,y,z) = u_{y_1} + yu_{y_2} + zu_{y_3} + y^2 u_{y_4} + yzu_{y_5} + z^2 u_{y_6} \tag{9}$$

$$u_z(x,y,z) = u_{z_1} + yu_{z_2} + zu_{z_3} + y^2 u_{z_4} + yzu_{z_5} + z^2 u_{z_6} \tag{10}$$

The Timoshenko beam theory (TBT) can be derived as a particular case of this formulation by considering only some terms of the TE1 expansion:

$$u_x = u_{x_1} + yu_{x_2} + zu_{x_3} \tag{11}$$

$$u_y = u_{y_1} \tag{12}$$

$$u_z = u_{z_1} \tag{13}$$

The Euler-Bernoulli beam theory can be derived by imposing a constraint on shear terms in order to obtain: $u_{x_2} = \frac{\delta u_x}{\delta x}$ and $u_{y_3} = \frac{\delta u_y}{\delta y}$.

C. Lagrange expansions

The Lagrange (LE) expansions have the following main features:

1) LE model degrees of freedom can be located directly above the physical surfaces of the CAD structure. This characteristic is particular relevant if the transverse section is not so simple;
2) Locally refined models can be easily built since Lagrange polynomials sets can be arbitrarily spread above the cross-section.

Lagrange polynomials are usually given in terms of normalized coordinates (fig.2). This choice is not compulsory but it offers several advantages. The simplest quadrilateral Lagrange polynomial is the four-point L4

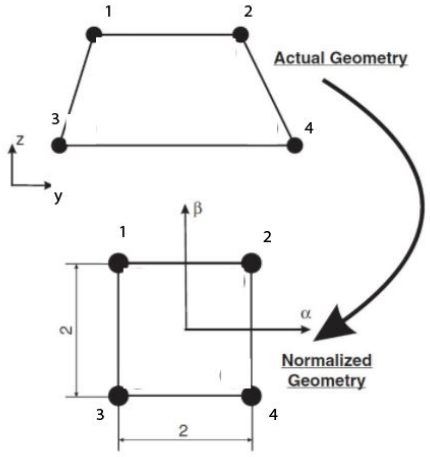

Figure 2. Four-node Lagrange element (L4) in actual and normalized geometry

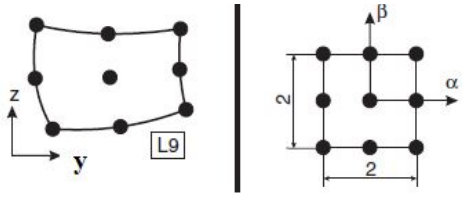

Figure 3. Four-node Lagrange element (L9) in actual and normalised geometry

set shown in fig. 2 whose polynomials are given by the following equation :

$$F_\tau = \frac{1}{4}(1 + \alpha\alpha_\tau)(1 + \beta\beta_\tau) \tag{14}$$

where α_τ and β_τ represent the normalised coordinates LE4 nodes.

The second possible L-set is given by L9 (fig.3) and its polynomials are the following ones:

$$F_{1,3,5,7} = \frac{1}{4}(\alpha^2 + \alpha\alpha_\tau)(\beta^2 + \beta\beta_\tau) \tag{15}$$

$$F_{2,4,6,8} = \frac{1}{2}\beta_\tau^2(\beta^2+\beta\beta_\tau)(1-\alpha^2)+\frac{1}{2}\alpha_\tau^2(\alpha^2+\alpha\alpha_\tau)(1-\beta^2) \tag{16}$$

$$F_9 = (1 - \alpha^2)(1 - \beta^2) \tag{17}$$

where α_τ and β_τ represent the normalised coordinates LE9 nodes.

D. Finite element approximation

Until this paragraph, we have focused on the expression of $F_\tau(y,z)$ that is not the only contribution to the displacement field. If the shape functions N_i are introduced, the unknown displacement $u_\tau(x)$ becomes:

$$u_\tau(x) = N_i(x) q_{i\tau} \tag{18}$$

where $q_{i\tau}$ are the degrees of freedom of the problem. Consequently, the displacement field and its virtual variation can be expressed as follows:

$$u = N_i(x) F_\tau q_{i\tau} \tag{19}$$

$$\delta u = N_j(x) F_\tau \delta q_{j\tau} \tag{20}$$

where indexes i and j indicate the longitudinal element nodes along the x-axis.

E. Governing Equations

The governing equation can be derived from the Principle of Virtual Displacement (PVD) that, if a free vibration analysis is performed, assumes the following form:

$$\delta L_{def} + \delta L_{ine} = 0 \tag{21}$$

where δL_{def} stands for the strain energy while δL_{ine} stands for the inertial work. Besides, L_{def} and L_{ine} are defined as follows:

$$\delta L_{def} = \int_V \delta \epsilon^T \sigma dV \tag{22}$$

$$\delta L_{ine} = \int_V \delta u^T \rho \frac{\delta^2 u}{\delta t^2} dV \tag{23}$$

By introducing the stress and strain definition given in the *Preliminary* section, L_{def} can be rewritten in the following way:

$$\delta L_{def} = \int_V \delta q_{js}^T [(N_j F_s D)^T C D F_\tau N_i] q_{i\tau} dV. \tag{24}$$

Therefore, it is possible to define a stiffness matrix $K^{ij\tau s}$ ([3x3]) where indexes τ and s can change from 0 to M, with M the number of terms of the transverse expansion F_τ:

$$K^{ij\tau s} = \int_V [(N_j F_s D)^T C D F_\tau N_i] dV \tag{25}$$

Besides, δL_{ine} can be written as follows:

$$\delta L_{ine} = \int_V \delta q_{js}^T [(N_j F_s \rho F_\tau N_i] \frac{\delta^2 q_{i\tau}}{dt^2} dV \tag{26}$$

from which the mass nucleo matrix $M^{ij\tau s}$ [3x3] can be derived:

$$M^{ij\tau s} = \int_V [(N_j F_s \rho F_\tau N_i] dV \tag{27}$$

After having assembled stiffness and mass matrices, the PVD can be rewritten by the following equation:

$$\delta q (M \frac{\delta^2 q}{\delta t^2} + Kq) = 0 \tag{28}$$

Finally, it is sufficient to solve the following eigenvalue problem to calculate the natural frequencies of the structure taken into consideration:

$$(-\omega_k^2 M + K) q_k = 0 \tag{29}$$

F. Assembling procedure

The previous sections have shown how the use of CUF allows the governing equations to be written in terms of fundamental matrices that can be used to build the global stiffness and mass matrices. The assembly procedure is shown in the fig.4. Five loops are necessary:

1) First and second loops are required to scan indexes τ ans s representing the expansion terms over the cross section. The result of these two loops will be the stiffness/mass matrices of a longitudinal node.
2) Third and fourth loops are required to scan the indexes i and j representing the longitudinal nodes of each beam element; the result at the end of this two loops will be the stiffness/mass matrix of a beam element along x-axis;
3) last loop is necessary to scan all the beam elements over the x-axis to obtain the global stiffness and mass matrices.

A specification is worth of mention and it concerns the case where Lagrange expansions are used. In fact, Lagrange expansions enable a locally refined mesh because cross-sections could be meshed by means of multiple LE elements. Multi-elements are generally adopted for the following purpose:

1) To refine the cross-section displacement field without increasing the polynomial expansions order
2) To refine locally the structure model.

If a multi-element cross-section is taken into account, it is necessary to add other two loops to the assembly procedure. An example of a multi-element cross-section

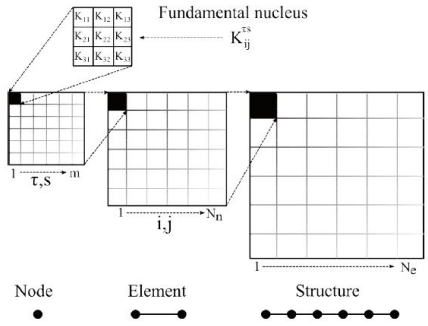

Figure 4. Assembly procedure to get global stiffness matrix

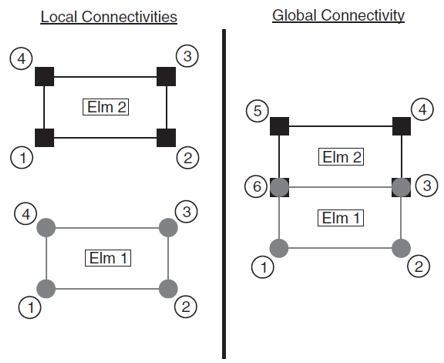

Figure 5. An example of two L4 elements assembled within a beam model

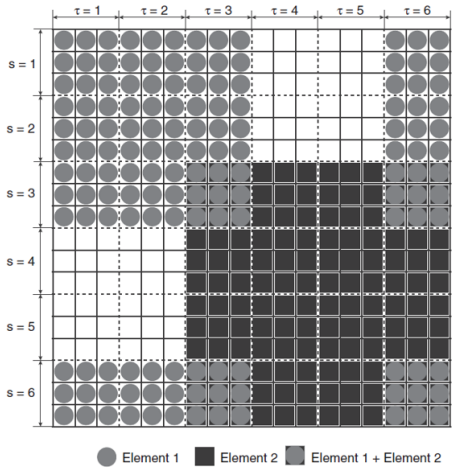

Figure 6. Assembly procedure of two L4 elements within a beam model

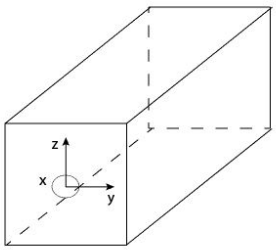

Figure 7. Square section beam and reference system

and of the assembling of its two LE elements is shown in fig.5 and fig.6.

Consequently, in this case, the global assembling procedure will be consist of the following loops:

1) First and second loops to scan indexes τ ans s to obtain the stiffness/mass matrix of a single LE cross-section element.
2) Third and fourth loop to scan all the LE elements into which the cross-section has been discretized; the result of this phase will be the stiffness/mass matrix of a single longitudinal node along $x-axis$.
3) Fifth and sixth loops to scan indexes i and j of a longitudinal element in order to calculate the stiffness/mass the element taken into account.
4) A last loop to scan all the longitudinal elements along x-axis in order to obtain the global stiffness/mass matrix.

IV. Numerical Results

This section investigates the accuracy of the 1D Refined Model compared to the traditional FEM 3D method. Firstly a convergence analysis has been performed on a simple square section beam. Secondly, the precision of the 1D Refined Method has been investigated for a thin-walled beam. Finally, this method has been applied to a simplified launcher model. Both Taylor expansions and Lagrange expansions have been used with several approximation order for validating the convenience od the 1D Refined Model. The results obtained by the TE and LE models are compared to those obtained using the MSC NASTRAN commercial code. The structures are built using aluminium with a Young modulus E of 75 GPa, poisson ratio ν of 0.33 and a density ρ of 2700 kg/m^3.

A. Convergence Analysis

A free-free square cross-section beam was considered in order to perform some convergence analysis. The

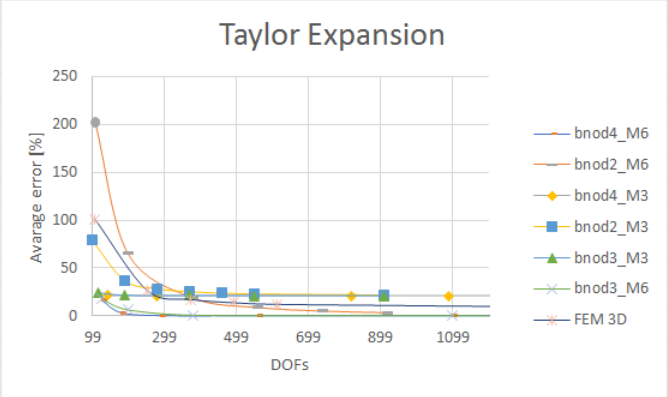

Figure 8. Convergence analysis of various Taylor expansions

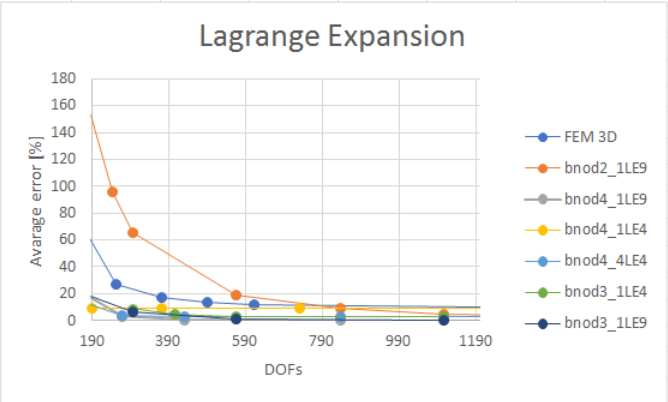

Figure 9. Convergence analysis of various Lagrange expansions

beam has been represented in fig.7: its length L is equal to 20 m and the edge h of the cross-section is 1 m. The assessments focused on the convergence of several expansions F_τ over the cross-section. TE models with several approximation orders were considered and, when LE model was applied, various discretizations over the cross-section were taken into account. Several beam elements were also used. In this context, we used the following abbreviations:

- *bnodN* to indicate that each beam element has N longitudinal nodes
- *TE-N* meaning that Taylor expansions are of order N
- *LE-N* to indicate that each Lagrange element of the cross-section has N nodes.

The average percentage error was calculated by performing the average between the first, second and third bending frequency errors. The reference bending frequencies were obtained by MSC NASTRAN Solid model with a very refined IsoMesh.

Fig.8 shows the convergence analysis performed by using different Taylor expansions over the cross-section. Several beam elements (bnod2, bnod3, bnod4) have also been used. The graph shows that the 1D Refined Model allows a better convergence compared to traditional FEM solid model and, in this case, the combinations *bnod3-M3* and *bnod3-M6* resulted very attractive.

Fig.9 shows the convergence study of Lagrange expansions where different transverse discretizations and several beam elements have been assessed: in this case, it resulted that the bnod4-1LE9 seems the most convenient as it converges before the other methods.

B. Thin-walled beam

A brief analysis has been carried out to investigate the 1D Refined method capability of performing a dynamic analysis of a thin-walled structure. In this context, a 20m long beam was considered with a ray of 1m. As far as LE expansions are concerned, different transverse discretizations were taken into account (fig.10) while TE precision was assessed by changing the approximation order N of the cross-section expansions. For all cases, a Beam element with 3 nodes was used (*bnod3*). The analysis was carried out by comparing the first and second frequencies obtained by 1D Refined Model to those obtained by MSC NASTRAN commercial code where a very refined mesh was used (DOFs 122409). Results are presented in table II and table III where the apexes indicate the relative percentage errors and ne_x represents the number of longitudinal beam elements.

Table II
FIST AND SECOND BENDING FREQUENCIES OF THIN-WALLED BEAM AND PERCENTAGE ERRORS THROUGH LAGRANGE EXPANSIONS

Mesh	ne_x	**DOFs**	f_1	f_2
A	13	1224	$28.691^{3.838\%}$	$72.725^{2.765\%}$
B	8	1224	$28.674^{3.896\%}$	$72.517^{3.043\%}$
C	8	1224	$29.817^{0.065\%}$	$74.899^{0.141\%}$

As table II shows, the combination bnod3-LE9 (*section C*) for the considered thin-walled beam results the most advantageous compared to the other meshes in fig.10. Moreover, table III that a greater approximation order N over the cross-section provides a more accurate solution. It is possible to notice that, for this geometry structure, the solution improvement provided by LE

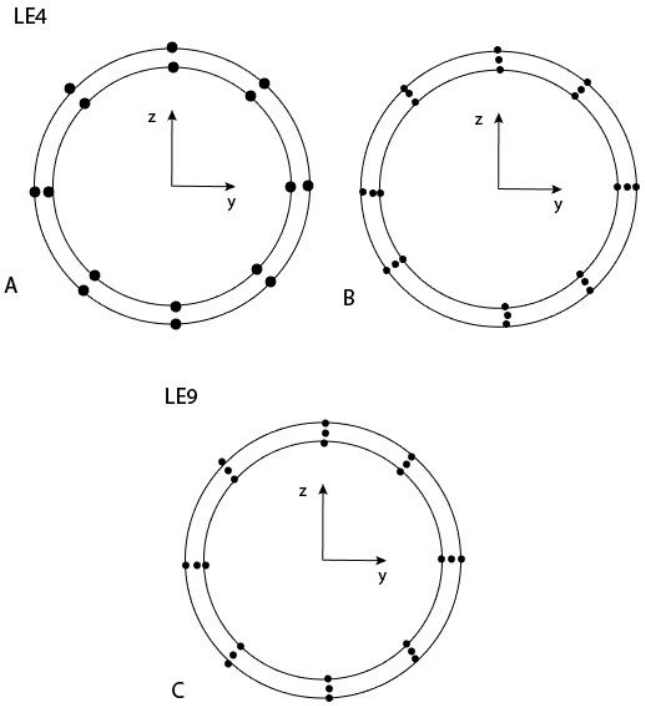

Figure 10. Cross-section discretization of a thin-walled beam

Table III
FIST AND SECOND BENDING FREQUENCIES OF THIN-WALLED BEAM AND PERCENTAGE ERRORS THROUGH TAYLOR EXPANSIONS

N	**M**	ne_x	**DOFs**	f_1	f_2
0	1	204	1227	$161.576^{441.549\%}$	$242.365^{224.047\%}$
1	3	68	1233	$36.49375^{22.315\%}$	$92.356^{23.483\%}$
2	6	34	1242	$30.221^{1.290\%}$	$77.813^{4.038\%}$
3	10	20	1230	$29.862^{0.088\%}$	$74.932^{0.186\%}$

models is greater and computationally cheaper than that provided by TE expansions.

C. Launcher Analysis

Through the 1D Refined Model the launcher has been modelled: its transverse section is represented in fig. 11. The entire structure is modelled by three main components: a central body, and two lateral boosters. As an approximation, each booster has been considered attached to the main body through a single point of attachment as shown in fig.11. The geometrical structure dimensions are shown in table IV. Also in this case, several combinations of BEAM elements and cross-section approximation orders have been analysed to perform an effective comparison. In this perspective, all the combinations have been performed maintaining the number of degrees of freedom DOFs almost constant

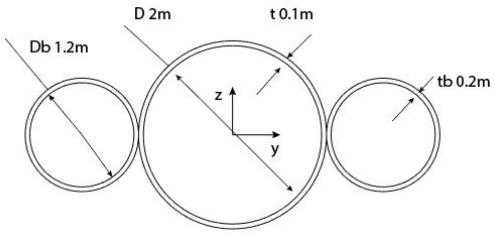

Figure 11. Launcher section

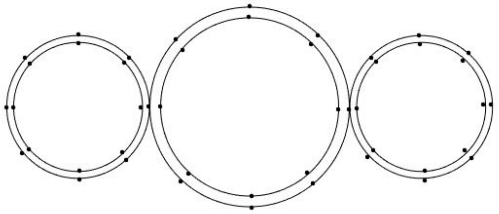

Figure 12. Launcher cross-section discretization with LE4 elements

and the results were compared to a very refined Nastran 3D model with 46815 DOFs. When LE elements were performed, fig.12 and fig. 13 show the cross-section discretizations used respectively for LE4 model and LE9 model. Results are shown in table V and represented from fig. 14 to 19.

Table IV
LAUNCHER'S GEOMETRICAL DIMENSIONS

Dimensions	**Value [m]**
D_b	1.2
D	2
t_b	0.2
t	0.1

Between the results, we included the solution 3D FEM with the same number of DOFs as for the other methods: in this case, the discretization shown in fig.12 has been used. Results illustrate that the 1D Refined Method,

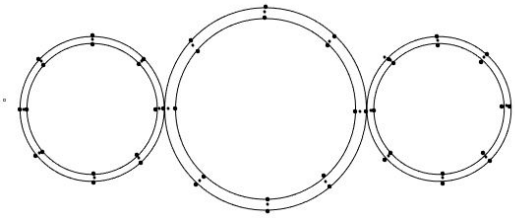

Figure 13. Launcher cross-section discretization with LE9 elements

Table V
FIST, SECOND AND THIRD GLOBAL FREQUENCIES OF LAUNCHERS PERCENTAGE ERRORS THROUGH LAGRANGE EXPANSIONS

	nod	n_{ex}	**DOFs**	f_1**[Hz]**	f_2**[Hz]**	f_3**[Hz]**
3D FEM	-	40	5658	$21.366^{1.964\%}$	$36.020^{3.225\%}$	$51.528^{2.590\%}$
LE4	3	20	5658	$20.957^{3.839\%}$	$35.987^{3.130\%}$	$51.344^{2.223\%}$
LE4	4	13	5934	$20.957^{3.839\%}$	$35.988^{3.131\%}$	$51.344^{2.223\%}$
TE3	3	94	5670	$22.112^{1.459\%}$	$49.797^{42.407\%}$	$55.037^{9.577\%}$
TE3	4	63	5700	$22.112^{1.459\%}$	$49.797^{42.407\%}$	$55.037^{9.577\%}$
TE2	3	156	5634	$22.210^{1.911\%}$	$49.973^{43.201\%}$	$56.111^{11.715\%}$
TE2	4	105	5688	$22.210^{1.911\%}$	$49.973^{43.201\%}$	$56.111^{11.715\%}$
LE9	3	13	5670	$21.814^{0.092\%}$	$37.276^{6.823\%}$	$51.077^{1.693\%}$
LE9	4	9	5580	$21.811^{0.078\%}$	$37.273^{6.814\%}$	$51.073^{1.684\%}$

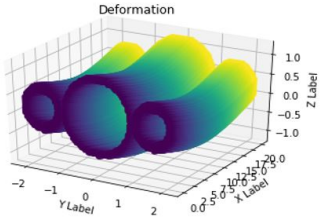

Figure 14. First global frequency by 1D Refined Model

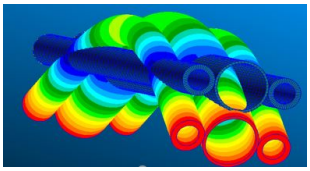

Figure 15. First global frequency by Solid NASTRAN Model

when Lagrange models are performed, provides solutions as accurate as those obtained through 3D Solid FEM. On the other hand, Taylor methods seem to be inconvenient for more complex cross-section geometries like the one taken into account for the launcher.

V. CONCLUSIONS

In this paper, different finite element models were compared for the free vibration analysis of several structures: a square-section beam, a thin walled cylinder and a launcher model. Two different one-dimensional refined models were derived by means of the Carrera Unified Formulation: one based on Taylor expansions and the other on the Lagrange expansions. The results were compared to those obtained by means of Solid FE models built using MSC NASTRAN commercial code. Through this study, it is possible to assess that Refined 1D Model with Lagrange Formulations provides results at least as accurate as those obtained by means of 3D Solid FEM. On the other hand Taylor formulations are not convenient for thin-walled structures or complex cross-section geometries but they could be very advantageous when simple structure like full beams or shells are analysed. We are currently applying this formulation to a reusable lunar launcher model. Further studies could take into account composite materials and gravity force.

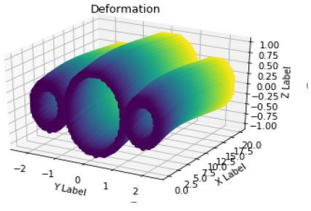

Figure 16. Second global frequency by 1D Refined Model

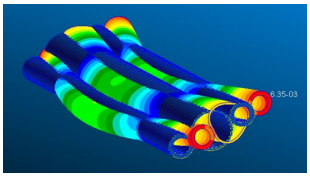

Figure 17. Second global frequency by Solid NASTRAN Model

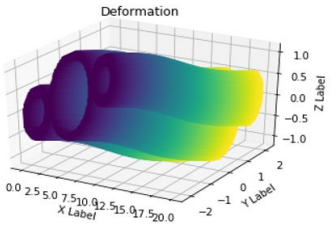

Figure 18. Third global frequency by 1D Refined Model

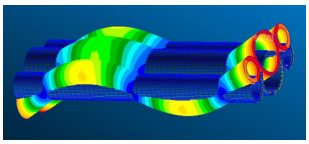

Figure 19. Third global frequency by Solid NASTRAN Model

REFERENCES

[1] Nali P. Petrolo M. Carrera E., Giunta G. Refined beam elements with arbitrary cross-section geometries. *Comput Struct*, 5(88):283–293, 2010.

[2] Petrolo M. Carrera E., Gaetano G. *Beam Structures, Classical and Advanced Theories*. John Wiley Sons, 2011.

[3] Petrolo M. Zappino E. Carrera E., Cinefra M. *Finite Element Analysis of Structures Through Unified Formulation*. John Wiley Sons, 2014.

[4] Carrera E. Analysis of fgm beams by means of classical and advanced theories. *Mech Adv Mater Struct*, 17(8):622–635, 2010.

[5] Carrera E. Theories and finite elements for multilayered plates and shells: a unified formulation with numerical assessment and benchmarking. *Arch Comput Methods Eng 2003*, 10(3):216–296, 2017.

[6] Carrera E. Belouettar S. Giunta G., Biscani F. Analysis of thin-walled beams via a one dimensional unified formulation through a navier-type solution. *Int J Appl Mech*, 3(3):407–434, 2011.

[7] W.C. Hurty. Dynamic analysis of structural systems using component modes. *AIAA jOURNAL*, 3(4):678–685, 1965.

[8] J.S. Przemieniecki. Matrix structural analysis of substructures. *AIAA Journal*, 1(1):138–147, 1963.